

Accepted Manuscript

Basalt powder as an eco-friendly filler for epoxy composites: Thermal and thermo-mechanical properties assessment

Danuta Matykiewicz, Mateusz Barczewski, Sławomir Michałowski



PII: S1359-8368(18)32223-6

DOI: <https://doi.org/10.1016/j.compositesb.2018.11.073>

Reference: JCOMB 6258

To appear in: *Composites Part B*

Received Date: 17 July 2018

Revised Date: 2 October 2018

Accepted Date: 15 November 2018

Please cite this article as: Matykiewicz D, Barczewski M, Michałowski S, Basalt powder as an eco-friendly filler for epoxy composites: Thermal and thermo-mechanical properties assessment, *Composites Part B* (2018), doi: <https://doi.org/10.1016/j.compositesb.2018.11.073>.

This is a PDF file of an unedited manuscript that has been accepted for publication. As a service to our customers we are providing this early version of the manuscript. The manuscript will undergo copyediting, typesetting, and review of the resulting proof before it is published in its final form. Please note that during the production process errors may be discovered which could affect the content, and all legal disclaimers that apply to the journal pertain.

Basalt powder as an eco-friendly filler for epoxy composites: Thermal and thermo-mechanical properties assessment

Danuta Matykiewicz¹, Mateusz Barczewski¹, Sławomir Michałowski²

¹ Polymer Processing Division, Institute of Materials Technology, Faculty of Mechanical Engineering and Management, Poznan University of Technology, Piotrowo 3, 61-138 Poznań, Poland; danuta.matykiewicz@put.poznan.pl, mateusz.barczewski@put.poznan.pl,

² Department of Chemistry and Technology of Polymers, Cracow University of Technology, Warszawska 24, 31-155 Kraków, Poland, spri@chemia.pk.edu.pl

Abstract

The aim of this study was to assess the influence of basalt powder on the thermo-mechanical properties of epoxy composites. The thermal stability was investigated through thermogravimetric analysis, flammability UL-94 test, and microcalorimetry. The degradation of the composite materials was evaluated using Kissinger's and Ozawa's methods. Moreover, the thermo-mechanical properties of the composites were determined through dynamic mechanical thermal analysis. Hardness was investigated with Shore D durometer. The results proved that basalt powder can be successfully used as an eco-friendly modifier for the epoxy resin. The thermo-mechanical properties of the composites improved with increased contents of this mineral filler. The presence of basalt powder retarded the degradation rate of the epoxy matrix as consequence the values of energy activation E_a for modified epoxy materials and HRR were higher than for the reference sample. Moreover, the addition of basalt powder improved stiffness and hardness of the composites.

Key words: basalt, epoxy, composites, thermo-mechanical properties, fire behavior

Introduction

The increasing accessibility of mineral deposits makes it possible to use them as pro-ecologic source of polymeric fillers. Epoxy resins, due to their good compatibility with various types of

powder fillers, can be successfully used as the matrix in composite materials. Moreover, as a result of the curing process, they achieve advantageous mechanical and thermal properties that allow their application in the building and automotive industries, and as coating materials [1,2]. The properties of cured epoxy resins depend on the chemical structure of the curing agents, curing conditions and the influence and reactivity of modifiers [3-6]. Therefore, the selection of a suitable filler in order to obtain composites with good chemical and heat resistance and good mechanical properties is the subject of many scientific papers [7-10]. Thermal stability and resistance of the epoxy resin may be improved by introducing organic and inorganic flame retardants or fillers which prevent thermal degradation of the composites. Notably, such modified materials must be safe for people and the environment. Flame retardants such as: clays [11,12], expandable graphite (EG) [13], metal hydroxides [14], melamine derivatives [15] and phosphorus derivatives [16,17] are successfully used as environmentally friendly modifiers. One of the mechanisms of flame retardation in modified polymers materials is the formation of a thick stable char layer, which acts both as a thermal insulator and as a barrier to oxygen [18,19].

Basalt fillers such as fiber and powder are produced during energy saving process from basalt rock [20]. Large deposits of this mineral are located in Poland, therefore finding an area for their application as eco-friendly fillers is an important technological and scientific issue. Basalt rock, classified as a igneous rock, contains mainly such minerals as plagioclase: $\text{Na}(\text{AlSi}_3\text{O}_8)$ - $\text{Ca}(\text{Al}_2\text{SiO}_8)$; pyroxene: $\text{XY}_2[(\text{Si}, \text{Al})_2\text{O}_6]$ (where X represents Ca, Mg, Fe^{2+} and Y represents Fe^{3+} , Al, Ti); and olivine: $(\text{Fe}, \text{Mg})_2\text{SiO}_4$ [21, 22]. Chopped basalt fibers are used in the building industry for producing mortar [22]. Long basalt fiber, mainly in form of woven fabric and mats, is applied as reinforcement for polymer composites with good mechanical properties [23]. However, to the best of the authors' knowledge, very few publications discuss the use of basalt powder as a low cost filler for improving the thermal resistance of the epoxy matrix [24,25]. Basalt powder has a fine grain structure and contains hard phases like diopside and augite. As a result, basalt composites present improved abrasion, wear and chemical resistance.

Therefore, the aim of this study was to verify the influence of basalt powder addition on thermal and thermo-mechanical properties of the epoxy composites. Thermal properties and degradation kinetics were determined through thermogravimetric analysis (TGA), microcalorimetry methods and UL94 test. Ozawa's and Kissinger's methods were applied to

obtain the kinetic parameters of thermal degradation. Thermo-mechanical properties were evaluated using dynamic mechanical thermal analysis. The structure of composites was characterized by Scanning Electron Microscopy. Moreover, the density and hardness of the composites were assessed.

Materials

The following components were used in this study: epoxy resin Epidian 6 (EP6) based on bisphenol A (BPA) (viscosity at 25°C; 10000 - 15000 mPas), curing agent – triethylenetetramine (Z1), both produced by CIECH Sarzyna S.A., Poland. Epoxy resin was mixed with Z1 at ratio 13 parts Z1 per 100 parts EP by weight. Basalt powder (BP) (Mine PGP BAZALT, Wilkowo, Złotoryia, Poland) were used as filler. According to data delivered by the producer, BP consists of: 49.5% SiO₂, 15% Al₂O₃, 9.6% CaO, 8.7% FeO, 6.8% MgO, 3.7% Fe₂O₃, 2.9% Na₂O, 1.2% K₂O, 0.4% P₂O₅, 0.2% MnO, 0.15% Mn, 0.0105% Zn, 0.0087% Cu, 0.0048% Co, 0.005% B, 0.00015% Mo. A detailed analysis of basalt powder particle size distribution is presented in our previous work [26]. On average, the size of the basalt particles was 10 µm.

Sample preparation

Epoxy matrix was mixed with a mechanical stirrer with 10; 20; 30; 40 wt% of basalt powder respectively to the total weight. Next, the compositions were mixed with the curing agent Z1. The epoxy composites were casted in a Teflon mold and cured at ambient temperature (20°C) for 24 h and post-cured at 80°C for 3 h. The samples were marked as E; E10B; E20B; E30B; E40B; adequately to the incorporated amount of basalt powder.

Thermogravimetry (TGA)

The thermal properties of modified epoxy/glass composites were determined by thermogravimetric analyses (TGA) with temperature range between 30°C and 900°C with various heating rates (i.e., 5, 10, 15, 20°C/min) under nitrogen atmospheres using a Netzsch TG 209 F1 apparatus. Approximately 5 mg samples were placed in ceramic pans. The initial decomposition

temperature T_{10%} was determined as the temperature at which the weight loss was 10%. The residual mass (W%) was defined at 900°C. Additionally, maximum thermal degradation temperatures were determined from derivative thermogravimetric (DTG) curves.

UL-94 horizontal burning test

The tests were carried out with the horizontal burning method (HB) using barrel-shaped samples sized 125x10x4 mm as per PN-EN 60695-11-10 standard. Burning time was measured and the dripping of burning material was monitored. According to the above observations, the samples' burning rate V was calculated, and on that basis the materials were classified (using UL 94 HB classifications).

Reflected light microscopy

Microscopic digital images of the samples after burning test were acquired using a MSt 130 (PZO Warszawa) reflected light microscope, equipped with Bresser MikroCam digital camera and magnification 2.83x.

Microcalorimetry

Average Total HR, kJ/g of the composites was determined using the pyrolysis combustion flow calorimetry (PCFC) technique, developed by Fire Testing Technology Ltd. (UK), using traditional oxygen depletion calorimetry. The samples were heated at a constant rate of temperature rise of 1°C/s in a pyrolyzer. Then the thermal decomposition products were swept from the pyrolyzer by an inert gas. Next, the gas stream was mixed with oxygen and entered a combustor at 900°C, which completely oxidized the products of decomposition. Nitrogen flow rate was 80 cm³/min and oxygen flow rate was 20 cm³/min.

Kinetics of thermal degradation

Ozawa's method is based on TGA curves recorded at various heating rates (β) [27]. It also includes the degree of conversion α , which is defined as the ratio of the actual weight loss to the total weight loss, $\alpha = (m_0 - m) / (m_0 - m_\infty)$, where m is the actual weight at time t (or at temperature T); m_0 is the initial weight, and m_∞ is the weight at the end of isothermal or non-isothermal experiments [28]. As a result, the rate of degradation da/dt , depends on the temperature and the weight of a sample, as presented by Eq (1).

$$\frac{d\alpha}{dt} = k(T) f(\alpha) \quad (1)$$

where: $k(T)$ is the rate constant and $f(\alpha)$ is a function of conversion. If we assume that $k(T) = A \exp(-E_a/RT)$ and $f(\alpha) = (1-\alpha)^n$, then Eq. (1) it can be described as present in Eq (2):

$$\frac{d\alpha}{dt} = A \exp\left(\frac{-E_a}{RT}\right) (1 - \alpha)^n \quad (2)$$

where: A is the pre-exponential factor; E_a is activation energy; R is gas constant; T is absolute temperature, and n is reaction order. After simple transformation we receive Eq. 3, which, based on the known degree of conversion α and heating rates β , will enable calculation activation energy values E_a .

$$\frac{d\alpha}{(1-\alpha)^n} = \left[\frac{A \exp(-E_a/RT)}{\beta} \right] dt \quad (3)$$

Based on equations 1-3 Ozawa's method allows to determine the activation energy from the plots of $\log \beta$ versus $1/T$ for defined value of α . The energy of activation can be calculated from the slopes of the lines according equation 4.

$$E_a = -slope * \frac{R}{0.457} \quad (4)$$

Kissinger method considers the maximum temperatures (T_m) appointed from DTG curves obtained at various heating rates [29]. In this method the temperature of maximum deflection in differential thermal analysis responds to the temperature at which the reaction rate is a maximum. Consequently, Eq. (3) is differentiated with respect to T and the resulting expression set to zero. Therefore activation energy was described in the equation below (5):

$$\frac{d[\ln(\beta/T_m^2)]}{d(1/T_m^2)} = \frac{-E}{R} \quad (5)$$

In this way, the activation energy can be calculated from a plot of $\ln(\beta/T_m^2)$ against $1/T_m$. The values of E_a were determined from the values of slope coefficient of a straight line presented by Eq. (6).

$$E_a = -slope * R \quad (6)$$

Density

The real density q_r of the composites was study based on PN-EN ISO 1183-1 standard by an immersion method using the AXIS AD 200 with a set to investigation the density of solids. The measurements were made in distilled water. What is more the theoretical density q_t were calculated as presented by Eq. (7) [30].

$$q_t = \frac{q_m \times q_f}{W_m \times q_f + W_f \times q_m} \quad (7)$$

Were q_t - theoretical density; q_m - matrix density; q_f - filler density; W_m - the weight content of epoxy matrix; W_f - the weight content of filler

In order to determine the void volume content U_v in the composites the Eq. (8) was applied [30].

$$U_v = \frac{q_t - q_r}{q_t} \quad (8)$$

Scanning Electron Microscopy (SEM)

The structure of composites was assessed by Scanning Electron Microscopy (SEM). The fracture surfaces of the samples were observed at the magnification of 1000 and digitally captured using a scanning electron microscope Zeiss Evo 40. The electron accelerating voltage of 12 kV was used. Prior to the tests, all the specimens were sputtered with a layer of gold.

Dynamic mechanical thermal analysis (DMTA)

The thermo-mechanical properties of the samples measuring 10 x 4 x 50 mm were determined using DMTA methods (Anton Paar MCR 301, Austria) in a torsion mode, operating at frequency $f = 1$ Hz in the temperature range 25-200°C, and at the heating rate 2°C/min. The position of $\tan \delta$ at its maximum was taken as the glass transition temperature (T_g).

Hardness

Shore D hardness was measured using a Sauter HBD 100-0 (Germany), according to PN-EN ISO 868.

Results and discussion

Thermal stability of composites

Thermogravimetric analysis (TGA) was conducted to investigate the thermal performance of composites. The TGA and DTG curves recorded with the heating rate of 10°C/min are presented in Fig 1 and Fig 2. Additionally, Fig 1 shows the TGA curves of pure basalt. Interestingly, basalt powder is very thermally stable and its residual mass was approximately 90 wt%. Detailed information on the degradation process, such as: ($T_{10\%}$) and ($T_{50\%}$), maximum intensity of thermal degradation temperatures (DTG), and residual mass, are presented collectively in Table 1. For all the investigated materials a single-step decomposition process was observed. For composites with a high amount of basalt powder the values of $T_{10\%}$ and $T_{50\%}$ were higher than for the reference sample. Moreover, introducing basalt powder into the epoxy matrix reduced their rate of degradation, which was proven by DTG analysis. Additionally, high amount of residual mass in composites may prevent the thermal degradation of material [31].

Table 1. TGA and DTGA data of the composites

Name	T10% [°C]	T50% [°C]	Residual mass [%]	DTG
E	345.4	373.2	7.5	365.7°C; 16.84%/min
E10B	343.4	370.4	13.2	361.3°C; 16.87%/min
E20B	346.4	381.8	22.6	363.7°C; 12.75%/min
E30B	346.0	381.9	30.91	360.2°C; 12.13%/min

E40B	352.5	391.8	36.04	365.3 °C; 13.04%/min
------	-------	-------	-------	----------------------

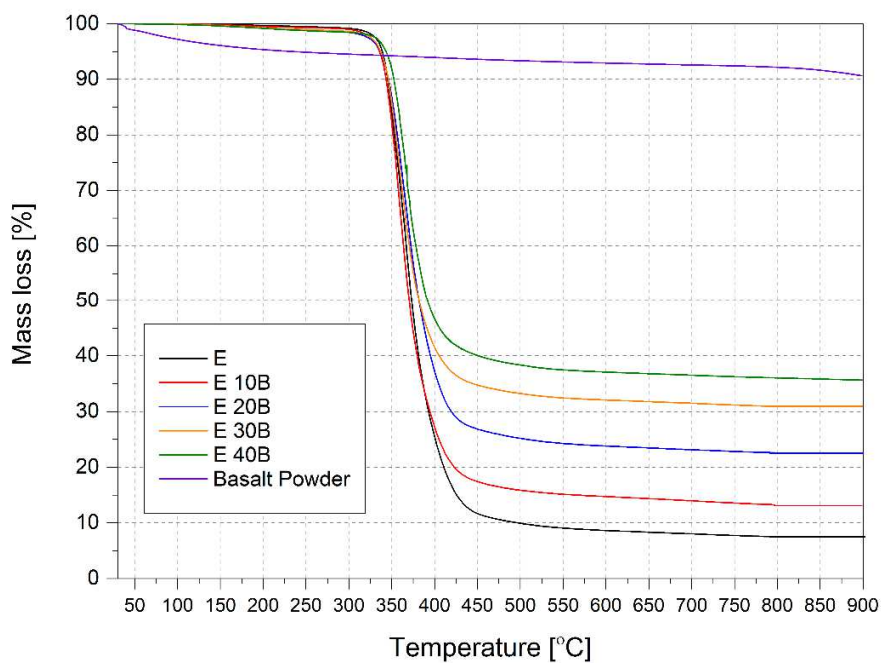


Fig. 1. TGA curves investigated composites recorded with heating rate of 10°C/min.

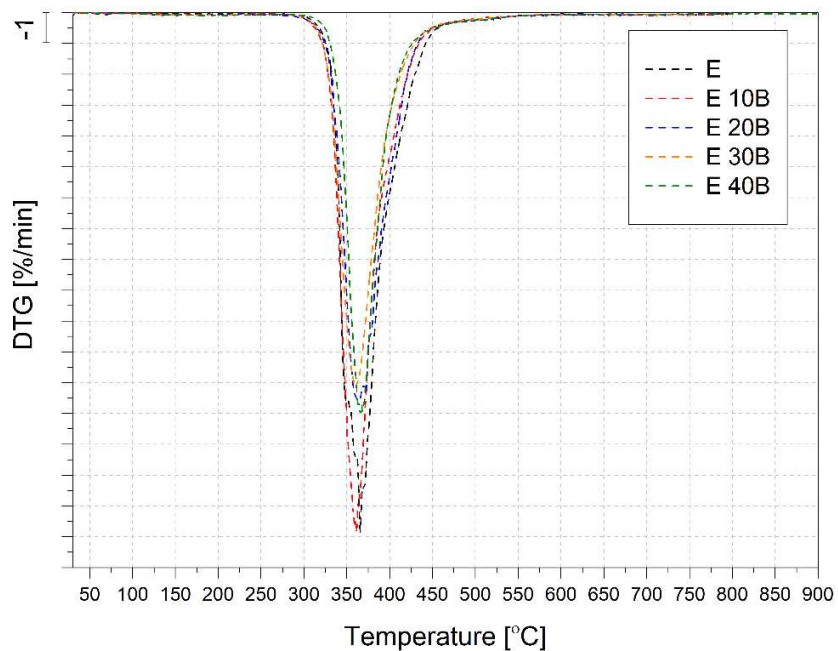


Fig. 2. DTGA curves investigated composites recorded with heating rate of 10°C/min.

UL-94 horizontal burning test

This method enables assessment of the flame spread in polymer materials, which may determine whether the material is safe in the event of fire. The results of the UL-94 burning test are presented in Table 2. The addition of basalt powder decreased significantly the burning rate (V) of composites, in comparison to the V of the neat sample. All samples with basalt powder were extinguished as soon as the burning process started, before reaching the measuring point. For samples with a high content of basalt powder (E 30B; E 40B), there were no dripping drops observed in the UL94 test. The presence of basalt powder in epoxy matrix led to a formation of char layer, which may have blocked the spread of the flame into polymer material, as shown in the Fig 3. Figure 3a shows microscopic photographs of the ash formed. It should be noted that the surface of E 30B and E 40B samples was slightly damaged compared to the reference sample.

Table 2. The flammability of composites according to UL-94 burning test

	E	E 10B	E 20B	E 30B	E 40B
V [mm/min]	16.5	self-extinguished	self-extinguished	self-extinguished	self-extinguished
Classification	HB40	HB40	HB40	HB40	HB40
Dripping drops	yes	yes	yes	no	no
Average Total HRR [kJ/g]	26.6±0.3	25.8±0.5	23.0±0.7	19.1±0.8	19.9±0.5

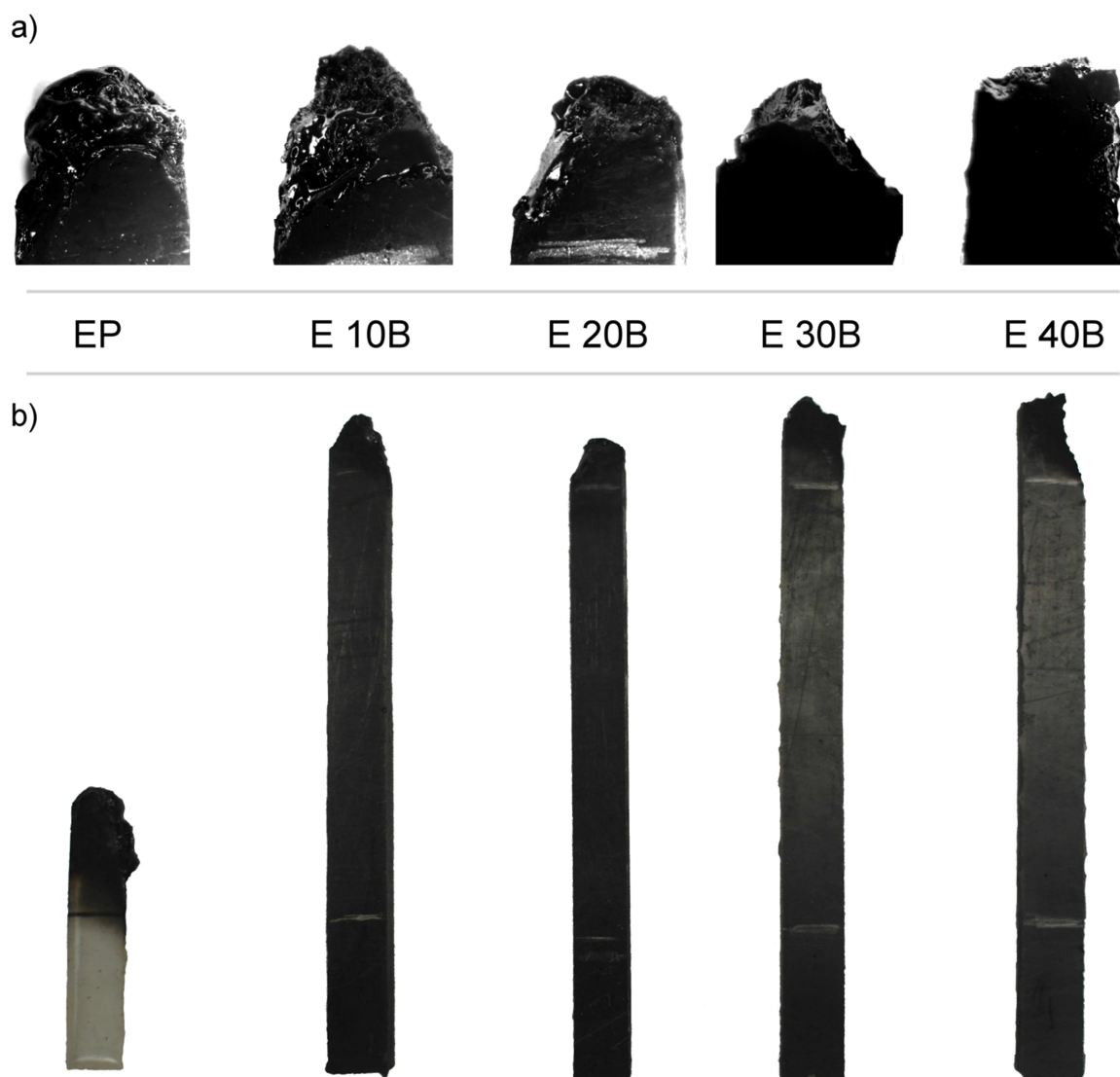


Fig.3. Microscopic images a) with magnification 2.83x and photographs b) of pure epoxy and composite samples after burning process.

Microcalorimetry

Microcalorimetry studies prove that basalt powder addition reduced the heat release rate (HRR) values during the burning process of the composites. The HRR values decreased simultaneously with BP content and for E 30B and E 40B samples those values were similar (Table 2). Those results are complementary to TGA and UL 94 study. The reduction of the heat release rate value for composites may confirm that basalt powder presence improves fire resistance of epoxy resin [32]. The microcalorimetry curves of the investigated composites show the significant

decomposition peak at the temperature range 360 - 380°C (Fig.4).The addition of the basalt powder into epoxy matrix result on shift of the HRR peak to higher temperatures, indicating that the composites have more stable thermal properties than reference sample.

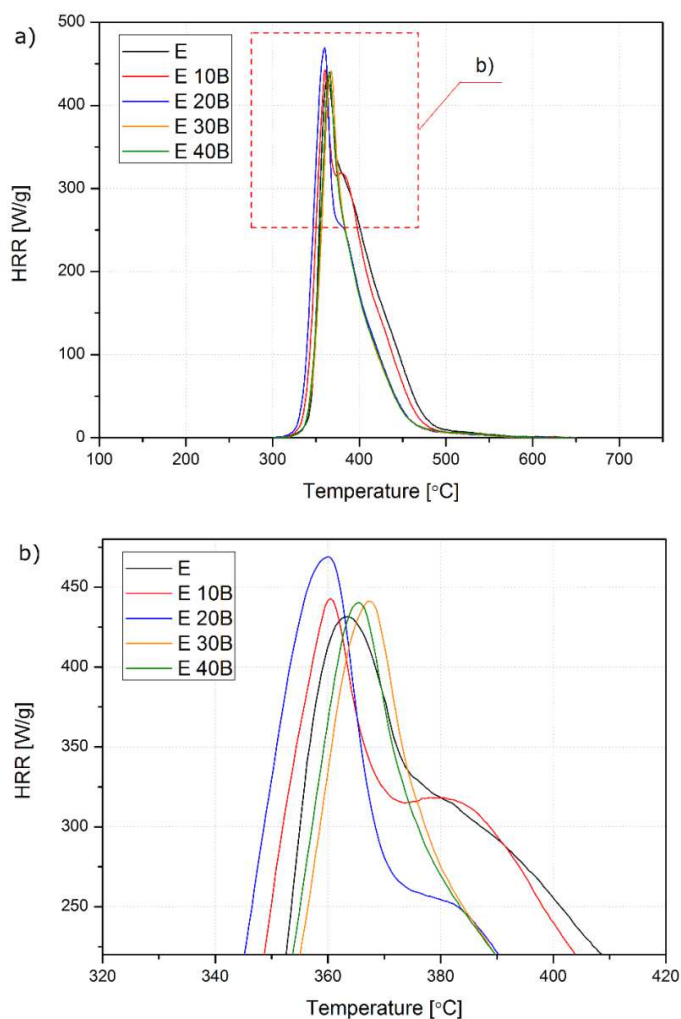


Fig 4. Microcalorimetry profiles for the investigated composites

Kinetics of thermal degradation in nitrogen atmosphere

As the Ozawa method requires, the TGA curves recorded at various heating rates for samples with a high amount of basalt powder are presented in Fig. 5, whereas Fig. 6 shows characteristic linear plots of $\log \beta$ versus $1/T$ for each value of α . In order to evaluate the effect of a powder filler on the process of epoxy matrix degradation, activation energies were calculated for all composites [32]. The relationship between the activation energies values and the degree of

conversion α for all the investigated materials are shown in Fig 7. The values of the activation energy E_a of thermal degradation process increases simultaneously with the degree of conversion of the samples. Introducing a high amount of mineral filler (30 and 40 wt%), improved the thermal resistance of epoxy material, which reflects their high values of E_a . This effect may be caused by the formation of a thick char layer on the degrading material surface and the presence of a high amount of very thermally stable basalt powder. For the EP40B sample the E_a values were much higher than the reference sample in the range of α 0,4-0,9 and for EP30B sample this phenomenon was observed in the range of α 0,5-0,9. The values of activation energy E_a of the thermal degradation process calculated by Kissinger's and Ozawa's methods are presented in Table 3. Importantly, both the results using Ozawa's method and Kissinger's method exhibit a similar tendency. Values of E_a increase with the increase in basalt powder content which also confirmed the improvement of thermal stability for studied materials.

Table. 3. The activation energy E_a of thermal degradation process calculated by Kissinger's and Ozawa's methods.

Name	E_a [kJ/mol] by Ozawa's method ($\alpha = 0,6$)	E_a [kJ/mol] by Kissinger's method
E	183.3	140.3
E10B	177.2	150.4
E20B	176.1	160.6
E30B	186.8	162.5
E40B	215.0	173.4

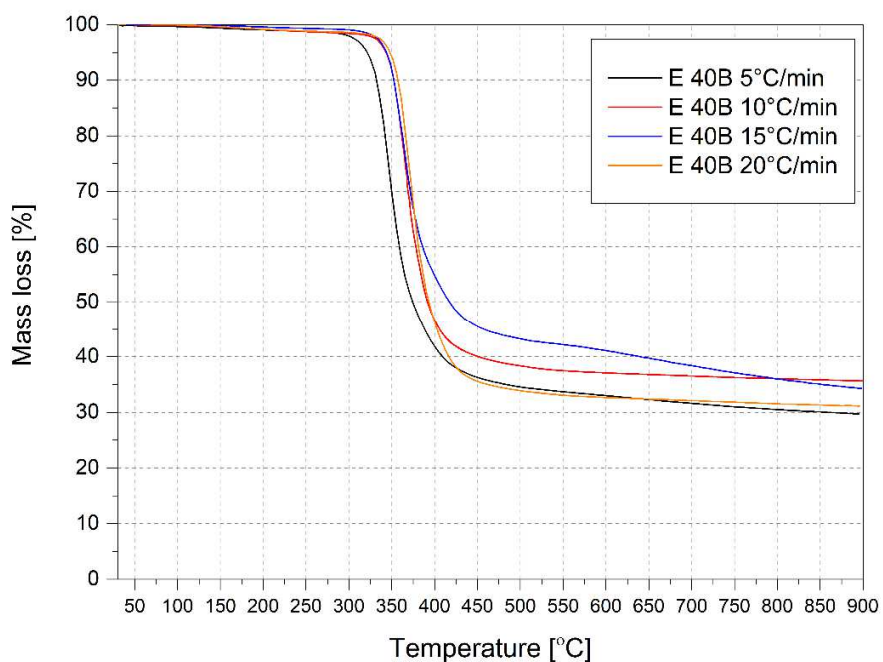


Fig. 5. TGA curves for sample E40B recorded at various heating rates.

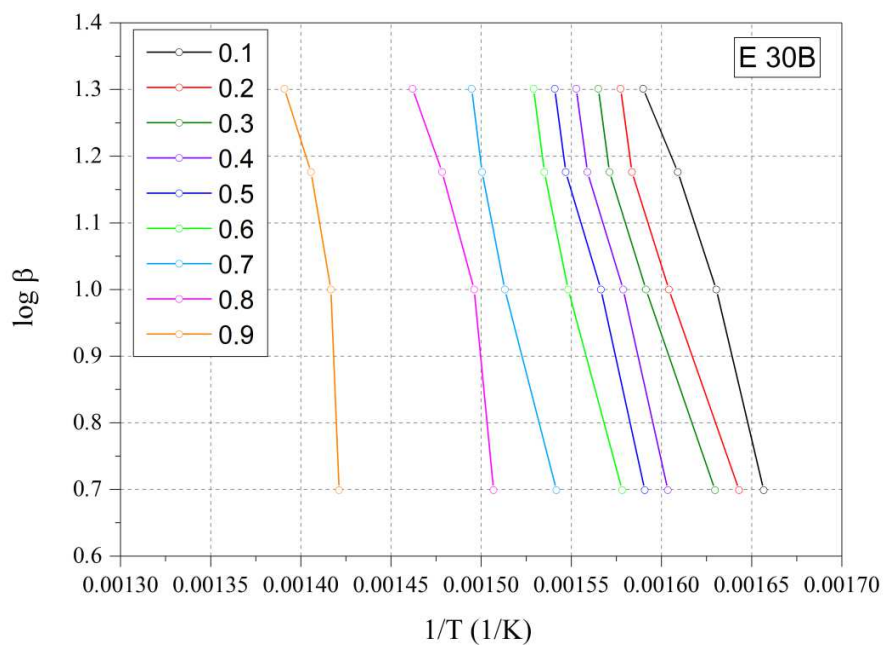


Fig. 6. Typical Ozawa plots for the thermal degradation for E 30B sample

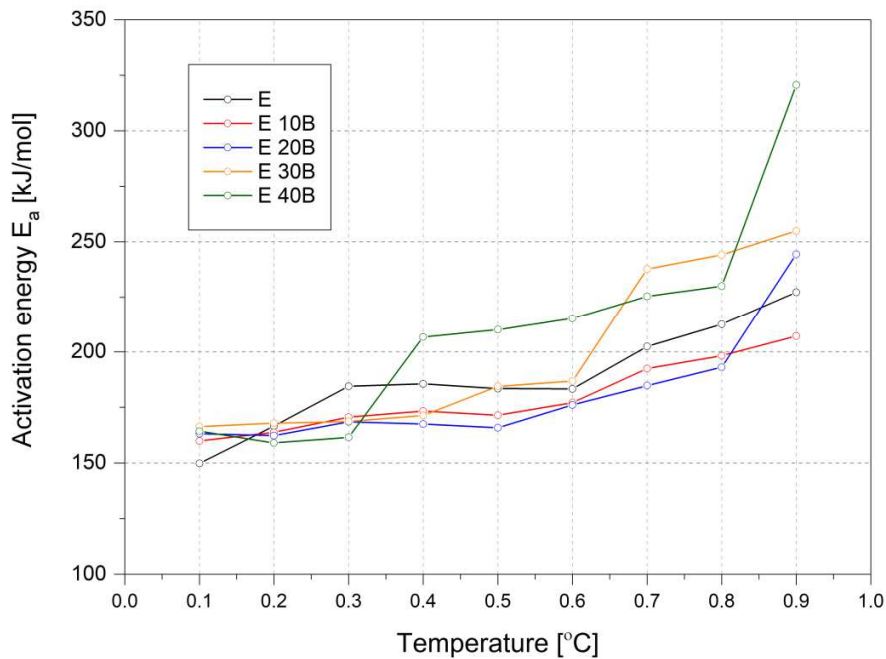


Fig. 7. The plot of the thermal degradation activation energy, E_a (kJ/mol), with various conversions by Ozawa's method.

Density

The composites density must be comprehensively analyzed with a view to the densities of individual components. Density of the basalt powder was determined pycnometer with ethanol and it was 2.8 g/cm^3 . During the production of the composites different voids may be occurred, caused by air or humidity presence. The values of real density, theoretical density and void volume content are collected in table 4.

Table. 4. Theoretical, real density and void volume content of the composites

Name	Theoretical [g/cm^3]	Real [g/cm^3]	Void volume content [%]
E	1.18	1.18	0
E10B	1.25	1.24	0.8
E20B	1.33	1.30	2.25
E30B	1.42	1.38	2.80
E40B	1.53	1.45	5.23

According to literature to define an excellent quality composite, the fraction of voids has to be $<1\%$, good quality composite has void fraction between 1% and 5% while void fraction $>5\%$ describe material with some defects [30]. In the presented SEM pictures no significant voids were observed, which may occur merely partly in the composites. The increase of density is a result presence in the composites the significant amount of the mineral filler with high density. Void volume content increasing with increased contents of basalt powder (Table 4). This effect may be result of air presence in composition with high amount of basalt filler and an increase in the viscosity of the composition from which the samples were cast.

Scanning Electron Microscopy (SEM)

In Figure 8, the SEM micrographs of the composites with different amounts of basalt powder are shown. For the composite samples with 10 and 20 wt% of BP well dispersed basalt powder was observed. In Fig. 8 d and e some agglomerates of basalt filler were noticed. Moreover, SEM micrographs of pure basalt powder (Fig. 9) proves that it may have some spheres in its structure. The structure of this mineral filler may be affected by its favorable interaction with polymeric materials.

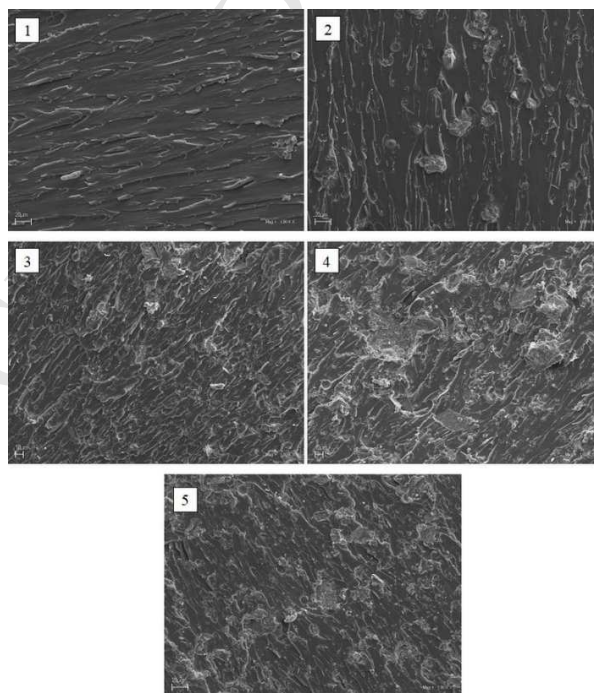


Fig. 8. SEM microphotographs of composite and reference sample a) E ; b) E 10B; c) E 20B;
d)E 30B; e)E 40B

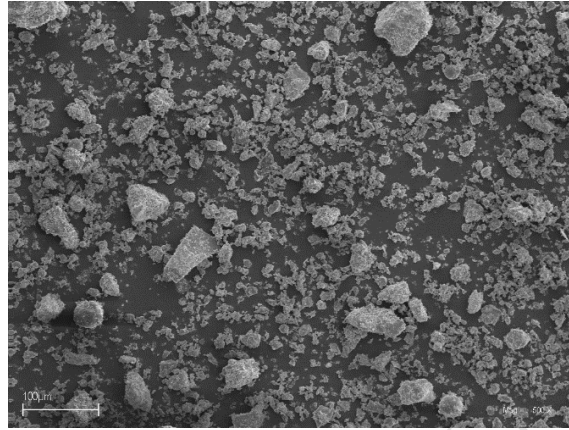


Fig. 9. SEM microphotographs of basalt powder.

Dynamic mechanical thermal properties

The properties of the thermoset composites materials depend on the curing conditions, type of the curing agent, interaction and the content of the filler. DMTA method allows to evaluate the following parameters: storage modulus G' , loss modulus G'' and mechanical loss factor ($\tan \delta$) versus temperatures T .

The values of the composites glass transition temperature (T_g) and storage modulus (G') recorded at various temperatures are presented in Table 5. As was shown in the plots of G' and $\tan \delta$ versus temperature, the introduction of basalt powder into epoxy resin changes their thermo-mechanical properties (Fig.10). In all cases the basalt powder addition improved the value of G' in the range of temperature 25-70°C. It is desirable that the introduction of the filler into epoxy matrix should improve their stiffness and mechanical properties. It can be concluded that the addition of the basalt powder improves the stiffness of the epoxy matrix. The same effect was confirmed by the results of the hardness test. In each case, except for sample EP20B, the glass transition temperature value was close to or higher than the reference sample T_g . Moreover, the shape of $\tan \delta$ curves presents the damping and molecular mobility of the polymer chains [34]. Introducing the mineral filler decreased $\tan \delta$ peak of the composites compared to pure epoxy

sample, which can be connected with lower damping properties of the composites and their lower impact strength [35]. Detailed analysis of the tan delta values also allows to evaluate the interaction between the composite components. According to the literature, good adhesion between filler and matrix reduces the polymer chains mobility and influences the decrease in the damping and the increase in the glass transition of the composites [33]. On the other hand, the width of the tan δ curves could be used to assess the homogeneity of the epoxy systems [35,36]. The addition of the basalt powder did not significantly affect the width of the composite curves. Moreover, crosslink density parameter V_e was calculated on a basis of equation (9), where E_r is storage modulus at ‘rubbery’ state, designated at $T_r = T_g + 30^\circ\text{C}$, and R is the universal gas constant [37,38]. It should be noticed, that the epoxy composites indicated a much higher V_e value than pure epoxy (Table 5).

$$V_e = \frac{E_r}{3RT_r} \quad (9)$$

Table 5. The values of composite storage modulus, glass transitions and crosslinking density obtained from DMTA.

Name	G' [GPa] at 30°C	T _g [°C]	tan δ peak	E _r at T _g + 30°C (MPa)	V _e (mol m ⁻³)
E	1170	126	0.75	16.40	19.50
E10B	1540	135	0.48	20.80	25.25
E20B	1600	121	0.46	23.80	27.97
E30B	1740	126	0.55	26.90	43.88
E40B	1800	131	0.55	39.60	47.64

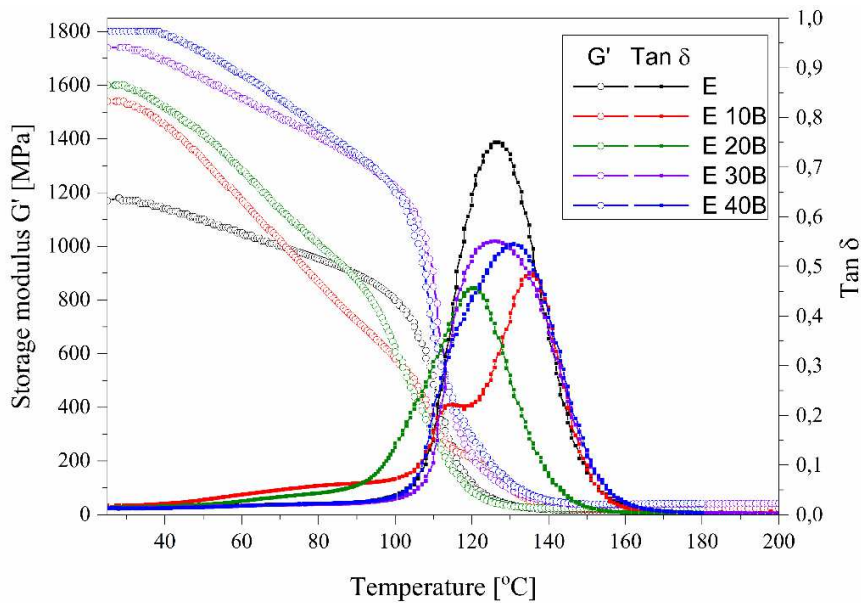


Fig. 10. The DMTA curves of the composites

Hardness

The addition of basalt powder favorably promoted the hardness of the modified materials. The relationship between the Shore D hardness and basalt powder content in epoxy materials is presented in Fig. 11. This effect is the result of the presence of hard rock-forming minerals in the basalt powder structure. According to the literature, basalt is a very hard material and reaches the hardness values between 5 to 9 on Mohr's scale [39]. The hardness of basalt rocks depends on the deposit they come from, because basalt was created of volcanic magma and flood volcanoes. These rocks are the result of solidified very hot fluid or semifluid material in contact with air [39].

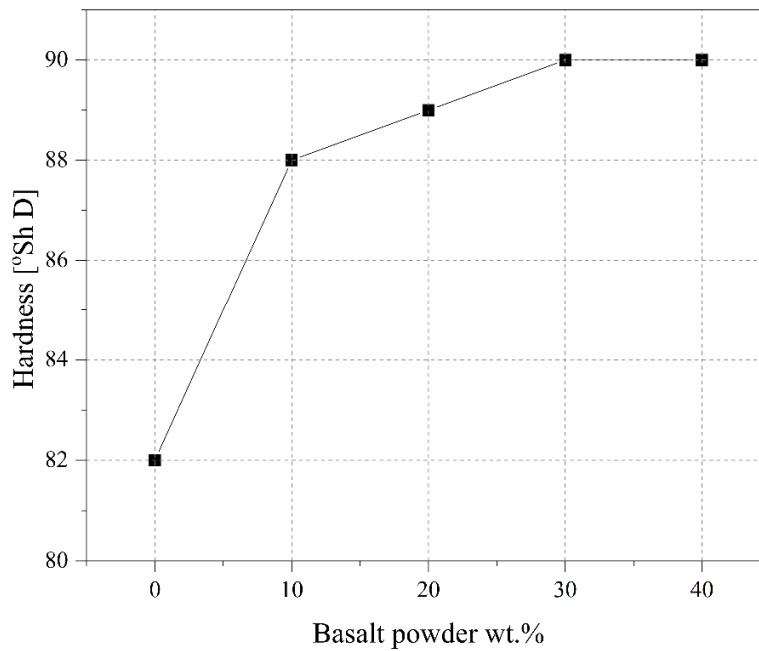


Fig. 11. Plot of the hardness value versus basalt powder content.

Conclusions

It can be concluded that epoxy composites modified with basalt powder indicate good thermal and thermo-mechanical properties. Thanks to the introduction of the eco- friendly basalt powder filler into epoxy matrix we obtained the protective effect on the epoxy materials against fire and high temperature. It was proven that high values of composites activation energy E_a and the heat release rate correspond to thermal degradation process. The calculation using Ozawa's and Kissinger's models gave similar results, which supports the correctness of the obtained data. Based on DTG curves, it can be stated that the presence of basalt powder retarded the degradation rate of epoxy matrix. Moreover, the addition of basalt powder improved stiffness and hardness of the composites. The values of composite storage modulus and crosslink density parameter were higher than the reference sample. In conclusion, the indicated thermomechanical properties of the composites were improved with the increase in the contents of the basalt powder. The results showed that basalt powder can be successfully used as an eco- friendly modifier for epoxy resin and assist in improving its thermal properties.

Acknowledgement

The presented research results, executed under the subject of No 02/25/DSPB/4520, were funded with grants for education allocated by the Ministry of Science and Higher Education in Poland.

References

1. Luciano G, Brinkmann A, Mahanty S, Echeverr  M. Development and evaluation of an eco-friendly hybrid epoxy-silicon coating for the corrosion protection of aluminium alloys. *Prog Org Coating* 2017; 110: 78-85.
2. Mahesh Babu S, Venkateswara Rao M. Effect of basalt powder on mechanical properties and dynamic mechanical thermal analysis of hybrid epoxy composites reinforced with glass fiber. *J Chinese Adv Mater Soc* 2018, <https://doi.org/10.1080/22243682.2018.1470030>.
3. Monteser n C, Blanco M, Laza JM, Aranzabe E, Vilas JL, Thickness effect on the generation of temperature and curing degree gradients in epoxy-amine thermoset systems. *J Therm Anal Calorim* 2018; 132:1867-1881.
4. Matykiewicz D, Barczewski M, Sterzy nski T. Morphology and thermomechanical properties of epoxy composites highly filled with waste bulk molding compounds (BMC). *J Polym Eng* 2015; 35: 805-811.
5. Oliwa R, Heneczkowski M, Oliwa J, Oleksy M, Mechanical strength of epoxy/organoclay/carbon fiber hybrid composites, *Polimery* 2017; 62: 658-665.
6. Mitu a K, Dutkiewicz M, Dudziec B, Marciniak B, Czaja K. A library of monoalkenylsilsesquioxanes as potential comonomers for synthesis of hybrid materials, *J Therm Anal Calorim* 2018; 132: 1545-1555.
7. Zatorski W, Sa asi nska K. Combustibility studies of unsaturated polyester resins modified by nanoparticles, *Polimery* 2016; 61; 815-823.
8. Zedler  , Colom X, Reza Saeb M, Formela K. Preparation and characterization of natural rubber composites highly filled with brewers' spent grain/ground tire rubber hybrid reinforcement. *Compos Part B Eng* 2018; 145: 182-188.
9. Choi YJ, Lee KM, Kim KS, Lee YS. Mechanical Properties of Epoxy Composites Reinforced with Carbon Nanotube and Oxyfluorinated Powdered-carbon Fiber. *Polymer- Korea* 2017, 41:835-843.

10. Salehi HR, Salehi M. Effect of TiO₂ nanoparticles on the viscoelastic and time-dependent behaviors of TiO₂/epoxy particulate nanocomposite. *J Polym Eng* 2017; 37, 185-196.
11. Zotti A, Borriello A, Ricciardi M, Antonucci V, Giordano M, Zarrelli M. Effects of sepiolite clay on degradation and fire behaviour of a bisphenol A-based epoxy. *Compos Part B Eng* 2015; 73: 139-148.
12. O Zabihi, M Ahmadi, S Nikafshar, K.C. Preyeswary, M. Naebe, A technical review on epoxy-clay nanocomposites: Structure, properties, and their applications in fiber reinforced composites. *Compos Part B Eng* 2018; 135: 1-24.
13. Jiao C, Zhang C, Dong J, Chen X, Qian Y, Li S. Combustion behavior and thermal pyrolysis kinetics of flameretardant epoxy composites based on organic-inorganic intumescent flame retardant. *J Therm Anal Calorim* 2015; 119:1759-1767.
14. Kong Q, Wu T, Tang Y, Xiong L, Liu H, Zhang J, Guo R, Zhang F. Improving Thermal and Flame Retardant Properties of Epoxy Resin with Organic NiFe Layered Double Hydroxide Carbon Nanotubes Hybrids. *Chin. J. Chem.* 2017; 35, 1875-1880.
15. Shen D, Xu YJ, Long JW, Shi XH, Chen L, Wang YZ. Epoxy resin flame-retarded via a novel melamine-organophosphinic acid salt: Thermal stability, flame retardance and pyrolysis behavior. *J Anal Appl Pyrolysis* 2017; 128: 54-63.
16. Huang Y, Yang Y, Ma J, Yang J, Preparation of ferric phosphonate/phosphinate and their special action on flame retardancy of epoxy resin *J Appl Polym. Sci* 2018, DOI: 10.1002/AP.46206.
17. Yang S, Wang J, Huo S, Wang M. Preparation and flame retardancy of an intumescent flame-retardant epoxy resin system constructed by multiple flame-retardant compositions containing phosphorus and nitrogen heterocycle. *Polym Degrad Stab* 2015; 119:251-259.
18. Kalali EN, Wang X, Wang DY. Multifunctional intercalation in layered double hydroxide: toward multifunctional nanohybrids for epoxy resin. *J Mater Chem A* 2016; 4: 2147-2157.
19. Kong Qi, Wu T, Zhang J., D.Y Wang Simultaneously improving flame retardancy and dynamic mechanical properties of epoxy resin nanocomposites through layered copper phenylphosphate. *Compos Sci Technol* 2018; 154: 136 -144.
20. Novitskii AG, Efremov MV. Technological aspects of the suitability of rocks from different deposits for the production of continuous basalt fiber. *Glass Ceram* 2013; 69: 409-412.

21. Kamiya S , Tanaka I, Imamura K, Sasaki H, Nakagawa N, Basalt fiber material, US Patent US 7,767,603 B2, Aug. 3, 2010.
22. Ralegaonkar R, Gavali H, Aswath P, Abolmaal S. Application of chopped basalt fibers in reinforced mortar: A review. *Constr Build Mater* 2018; 164: 589-602.
23. Fiore V, Scalici T, Di Bella G, Valenza A. A review on basalt fibre and its composites. *Compos Part B Eng* 2015; 74: 74-94.
24. Raja MA, Manikandan V, Amuthakkannan P, Rajesh S, Balasubramanian I. Wear resistance of basalt particulate-reinforced stir-cast Al7075 metal matrix composites, *J Aust Ceram Soc* 2018; 54:119-128.
25. Mishra R, Jamshaid H, Militky J. Basalt nanoparticle reinforced hybrid woven composites: Mechanical and thermo-mechanical performance. *Fiber Polym* 2017; 18: 2433-2442.
26. Matykiewicz D, Barczewski M, Knapski D, Skórczewska K. Hybrid effects of basalt fibers and basalt powder on thermomechanical properties of epoxy composites, *Compos Part B Eng* 2017; 125:157- 164.
27. Ozawa T, *Bull Chem Soc Jpn* 1965; 38:1881.
28. Chiang CL, Chang RC, Chiu YC. Thermal stability and degradation kinetics of novel organic/inorganic epoxy hybrid containing nitrogen/silicon/phosphorus by sol-gel method, *Thermochim Acta* 2007; 453: 97-104.
29. Kissinger HHE. *Anal Chem* 1957; 29: 1702.
30. Agarwal BD, Broutman LJ. *Analysis and Performance of Fibre Composites*. JohnWiley & Sons (1990).
31. Xu W, Wang X, Liu Y, Li W, Chen R. Improving fire safety of epoxy filled with graphene hybrid incorporated with zeolitic imidazolate framework/layered double hydroxide. *Polym Degrad Stab* 2018; 154: 27-36.
32. Zhou K, Tang G, Gao R, Jiang S. In situ growth of 0D silica nanospheres on 2D molybdenum disulfide nanosheets: Towards reducing fire hazards of epoxy resin. *J Hazard Mater* 2018; 344: 1078-1089.
33. Fiore V, Di Bella G, Scalici T, Valenza A. Effect of plasma treatment on mechanical and thermal properties of marble powder/epoxy composites *Polym Compos* 2018; 39: 309-317.

34. Zabihi O, Hooshafza A, Moztafzadeh F, Payravand H, Afshard A, Alizadehe R, Isothermal curing behavior and thermo-physical properties of epoxy-based thermoset nanocomposites reinforced with Fe₂O₃ nanoparticles, *Thermochim Acta* 2012, 527, 190-198.
35. Saba N, Jawaid M, Alothman OY, Paridah MT. A review on dynamic mechanical properties of natural fibre reinforced polymer composites, *Constr Build Mater* 2016; 106: 149 -159.
36. Johansson M, Glauser T, Rospo G, Hult A. Radiation curing of hyperbranched polyester resins. *J Appl Polym Sci* 2000; 75: 612-618.
37. Gerard JF, Galy J, Pascault JP, Cukierman S, Halary JL. Viscoelastic response of model epoxy networks in the glass transition region *Polym Eng Sci* 1991; 31:615-621.
38. Nakka JS, Jansen KMB, Ernst LJ, Jager WF. Effect of the epoxy resin chemistry on the viscoelasticity of its cured product, *J Appl Polym Sci* 2008; 108:1414-1420.
39. Singha K, A Short Review on Basalt Fiber. *International Journal of Textile Science* 2012, 1(4): 19-28.